Thin Solid Films 517 (2009) 1895–1898

Contents lists available at ScienceDirect

Thin Solid Films

journal homepage: www.elsevier.com/locate/tsf

Oxidation of magnetron sputtered La-Si thin films for solide oxide fuel cell electronlytes

J.C. Oliveira [a,*], D. Horwat [b], A. Billard [c], A. Cavaleiro [a]

[a] SEG-CEMUC, Mechanical Department, University of Coimbra, Rua Luís Reis Santos, 3030-788 Coimbra – Portugal
[b] Laboratoire de Science et Génie des Surfaces (UMR 7570), Ecole des Mines, Parc de Saurupt - F 54042 Nancy Cedex, France
[c] Laboratoire d'Etudes et de Recherches sur les Matériaux, les Procédés et les Surfaces, UTBM, Université de Technologie de Belfort-Montbéliard, 90010 Belfort, France

ARTICLE INFO

Article history:
Received 27 December 2007
Received in revised form 26 September 2008
Accepted 29 September 2008
Available online 11 October 2008

Keywords:
Lanthanum silicate
Sputtering
Oxidation
Electrolyte

ABSTRACT

La-Si thin films were deposited on stainless steel substrates by magnetron sputtering from pure La and Si targets. The Si/(Si+La) atomic ratio in the films was varied from 43.2 to 59.3% by adjusting the discharge current on the La target. The films had a homogeneous chemical composition down to the substrate and sharp interfaces. Annealing the films in air at 1173 K promotes the formation of apatite-structure $La_{9.33}Si_6O_{26}$ and the diffusion of different species from the film to the substrate and vice-versa, resulting in broadening the interfaces. X-Ray diffraction showed that all the as-deposited films had an amorphous structure. The formation of the $LaSi_2$ phase at intermediate temperatures was observed for the films deposited with higher Si contents while the films deposited with lower Si contents remained amorphous up to the start of the apatite structure crystallization process. The lanthanum silicate apatite-like phase ($La_{9.33}Si_6O_{26}$) was obtained only after annealing at 1173 K, excepted for the film with the lower Si content which is already partially crystallized after annealing at 1073 K. Quite pure $La_{9.33}Si_6O_{26}$ was obtained only after annealing the film with the highest Si content (Si/(Si+La)=59.3%) although the theoretical Si/(Si+La) atomic ratio for apatite structure lanthanum silicate is 39%. For the other films, La_2O_3 was always detected when the lanthanum silicate phase was formed. Both phenomena clearly resulted from the strong diffusion of silicon excess towards the stainless steel substrate.

1. Introduction

Solid oxide fuel cells (SOFCs) have grown in recognition as a viable high temperature fuel cell technology [1,2]. However, high temperatures in SOFCs (1073-1273 K) impose stringent requirements on the cell component materials which result in high material costs for interconnect and sealing materials and cause system degradations due to interface reactions and high thermal cycling stress. Reducing the operating temperature of SOFCs will decrease the fuel cell power density because of the decrease in both the electrolyte ionic conductivity and the catalytic activity of the cathode [3].

Decreasing the electrolyte thickness to the micrometer range and, therefore, the ohmic drop in the electrolyte has long been recognized as a straightforward way to achieve intermediate temperature SOFCs (IT-SOFCs) [4,5]. Several works about the synthesis of thin and dense conventional yttria-stabilised zirconia (YSZ) electrolyte coatings on porous anode substrates by sputtering processes [6,7] have already been published.

Another route to achieve IT-SOFCs is the development of electrolyte materials with ionic conductivity higher than that of the conventional YSZ at moderate temperatures [4,8]. Some oxide ion conductor electrolytes such as doped ceria or lanthanum gallate show conductivities comparable to, or better than, YSZ at 873 K, and are thus potential electrolytes for economic feasible fuel cells [4,5,9,10]. Recently, lanthanum silicate materials ($La_{9.33}Si_6O_{26}$) with an apatite-like structure have attracted considerable interest as potential low temperature electrolyte materials [11,12].

This study is part of a work which aims at applying the sputtering technology to the development of apatite-like lanthanum silicate electrolytes for IT-SOFCs. Two approaches could be used to reach this objective: the deposition La-Si films and subsequent controlled oxidation of the films or the deposition of La-Si-O films followed by annealing to produce the apatite-type structure [13]. This study focuses on the formation of apatite-like lanthanum silicate by oxidation of La-Si films as-deposited by magnetron sputtering.

2. Experimental details

La-Si films were deposited by magnetron sputtering from pure La and Si targets using an Alcatel SCM 640 deposition system. Before each deposition, the sputtering chamber was pumped down via a turbo-

* Corresponding author.
E-mail addresses: joao.oliveira@dem.uc.pt (J.C. Oliveira), david.horwat@mines.inpl-nancy.fr (D. Horwat), alain.billard@utbm.fr (A. Billard), albano.cavaleiro@dem.uc.pt (A. Cavaleiro).

0040-6090/$ – see front matter © 2008 Elsevier B.V. All rights reserved.
doi:10.1016/j.tsf.2008.09.100

molecular pump allowing a base vacuum of about 10^{-4} Pa. The targets (200 mm in diameter) were positioned at 130 mm from the substrate holder axis and powered by pulsed direct current Advanced Energy Pinnacle+supplies operated at a fixed frequency of 50 kHz (t_{off}=5 μs). The Si target power was maintained constant at 1000 W in all depositions whereas the La target power was varied from 250 to 650 W. All films were deposited on glass slides and AISI 430 stainless steel substrates with a fix run duration of one hour. Pure Argon (99.99%) was used as discharge gas with a constant flow rate of 20 sccm in all experiments, resulting in a deposition pressure of about 0.1 Pa.

The chemical composition of the coatings was determined by electron probe microanalysis (EPMA) using a Cameca SX-50 equipment with an acceleration voltage of 15 keV and LaB_6 and Si standards. Each presented value is the result of at least 5 measurements. Elemental depth profile analysis was performed by secondary neutral mass spectroscopy (SNMS) on a SimsLab-VG apparatus using Ar^+ ions accelerated to 8 kV and typical currents in the range 300-500 nA. The sputtered atoms where post-ionised by SNMS electrons for the Mass Spectroscopy analysis. Calibration of the SNMS yields of La, Si and O was performed using the EPMA results. The structure of the coatings was studied by hot X-ray diffraction (XRD) using a Phillips diffractometer operated in Bragg-Brentano configuration with Co(Kα) radiation. The La-Si films deposited on stainless steel substrates and annealed in-situ at a constant rate of 30 K/min under ambient air using a Pt filament. The X-ray diffraction patterns were acquired at room temperature, 873, 973, 1073 and 1173 K.

3. Results

The chemical composition measured by EPMA on the La-Si films is shown in Fig. 1 as a function of the power applied to the La target. The Si content decreases almost linearly with increasing the La target power, resulting in the deposition of thin films with Si/(La+Si) atomic ratios between 43.2 and 59.3%.

The SNMS depth profile analysis of the as-deposited films with Si/(La+Si) ratios of 43.2 and 49% are shown in Fig. 2. The chemical composition of the films was calculated from the SNMS signal intensities using the EPMA results shown in Fig. 1 for calibration. Both films have a homogeneous chemical composition down to the substrate and sharp interfaces. As expected, the Fe/Cr ratio signal intensity was in agreement with the value expected for the AISI 430 stainless steel substrate. The oxygen content in the films is negligible within the experimental error margin.

The SNMS depth profiles obtained after annealing the films at 1173 K for one hour in ambient atmosphere are shown in Fig. 3. The annealing process promotes the diffusion of the different species from the film to the substrate and vice-versa, resulting in the broadening of the interfaces. The high oxygen content measured after annealing shows that a significant oxidation of the films was achieved. Moreover, the oxygen concentration is close to 70 at. % which is consistent with the formation of the lanthanum silicate apatite-like phase ($La_{9.33}Si_6O_{26}$). This hypothesis is also supported by the variations of the La to Si atomic ratios as a result of the annealing

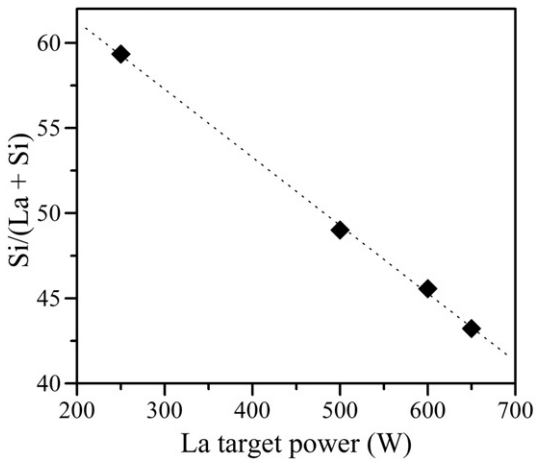

Fig. 1. Si/(Si+La) atomic ratio in the films as a function of the La target power.

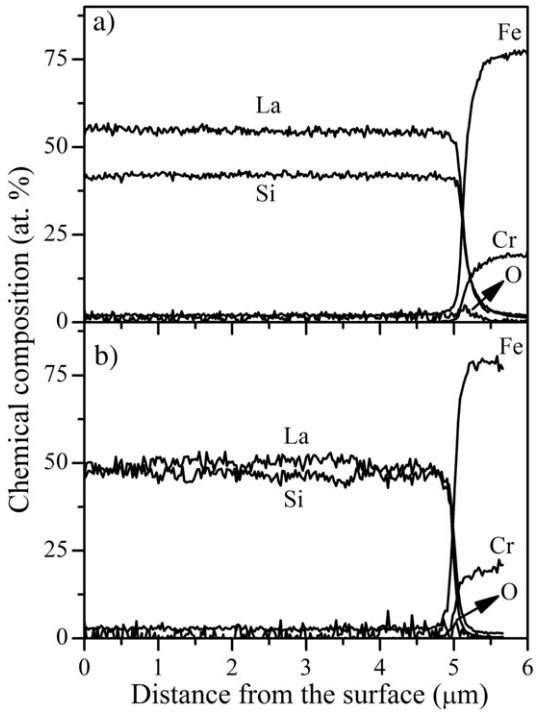

Fig. 2. SNMS depth analysis of the as-deposited films with a Si/(Si+La) atomic ratio of: a) 43.2 and b) 49.%.

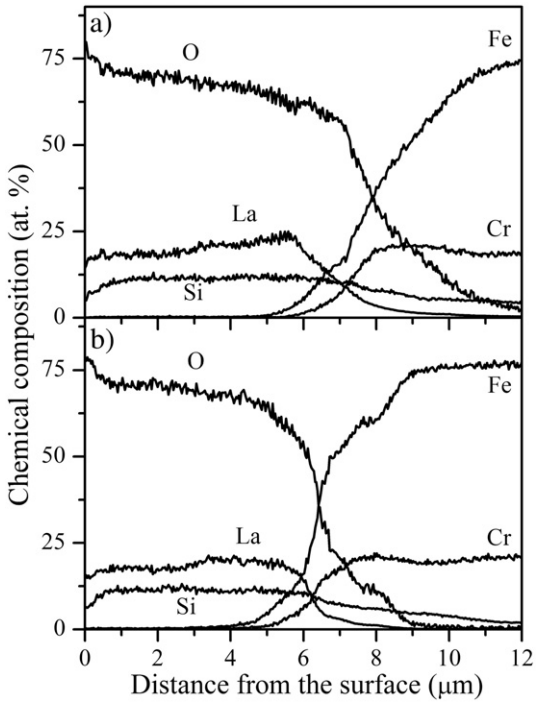

Fig. 3. SNMS depth analysis of the films deposited with a Si/(Si+La) ratio of: a) 43.2% and b) 49% after annealing 1 h at 1173 K.

process. Before annealing, the Si/(Si+La) atomic ratios in the films were substantially different (43.2 and 49% - see Fig. 2) while after annealing the films present similar Si/(Si+La) atomic ratios which are close to the value expected for the lanthanum silicate apatite-like phase (about 39%). A striking feature that can be observed in both graphics in Fig. 3 is the high silicon content visible within the substrate, in opposition to the La atomic content which quickly decreases at the interface. The excess silicon resulting from the oxidation of the deposited films, which have a higher Si content than the lanthanum silicate apatite-like phase before annealing, is rejected at the oxidation interface and finally incorporated into the substrate itself. Such a phenomenon has already been observed during high temperature annealing in air of Cr-Si-N coatings [14] and is attributed to the strong affinity of Si with AISI 430 stainless steel. Therefore, if atomic diffusion of Si is allowed in a given substrate for La-Si films, the apatite–like phase is expected to form over a wide range of compositions upon air annealing.

Fig. 4a shows the XRD patterns of the La-Si coatings with a Si/(Si+La) ratio of 59.3%. The as-deposited film has a quasi-amorphous structure as it can be concluded from the broad diffraction peaks detected by X-ray diffraction around $2\theta \approx 36$ and 57°. Annealing the film at 873 K promotes its crystallization and the formation of the $LaSi_2$ phase [15] which is thermodynamically stable at this temperature [16]. However, the LaSi phase, which is also predicted by the equilibrium La-Si phase diagram [16] is not formed upon annealing of the coating containing 59.3 at.% Si. $LaSi_2$ remains the only phase detected after annealing at 973 K. The sharpening of the diffraction peaks indicates that the crystallization process progresses while increasing the annealing temperature. The $LaSi_2$ phase is still observed after annealing at 1073 K. However, the low intensity of the diffraction peaks, as compared with that of the patterns obtained at lower annealing temperatures, and the presence of a broad peak centred around $2\theta \approx 33°$ indicate that the films are progressively becoming amorphous. Annealing performed at 1173 K leads to a complete crystallization of the film, resulting in the formation of the quite pure lanthanum silicate apatite-like phase [17].

The La-Si film deposited with a Si/(Si+La) ratio of 49% also has a quasi-amorphous structure in the as-deposited state (see Fig. 4b). The quite similar broad diffraction peaks already observed for the film with Si/(Si+La) ratio of 53.2 at.% are also detected by X-ray diffraction. Even if the film chemical composition lies in the $LaSi+La_5Si_4$ phase mixture compositional range of the La-Si phase diagram [16], no equilibrium phases were detected by X-Ray diffraction after annealing up to 1073 K. Instead, a broad peak centred around $2\theta = 33°$ appears in the diffraction pattern at 873 K along with weak diffraction peaks corresponding to the $LaSi_2$ phase. The broad diffraction peak is the only feature present in the diffraction pattern after annealing up to 1073 K. Once again, annealing at 1173 K leads to the formation of the lanthanum silicate apatite-like phase. However, besides the $La_{9.33}Si_6O_{26}$ phase diffraction lines two additional peaks indexed as the La_2O_3 phase [18] are detected. The presence of lanthanum oxide despite a coating composition presenting an excess of Si owing to the formation of apatite is clearly in relation with the Si diffusion into the stainless steel substrate. Note that the presence of diffraction peaks corresponding to the substrate and its oxidation shows that part of the film was detached upon annealing at 1173 K.

The evolution of the X-ray diffraction patterns upon the annealing of the film deposited with a Si/(Si+La) ratio of 45.6% (Fig. 4c) is similar to that obtained with the film deposited with 49% Si. However, two main differences were observed. First, the formation of the $LaSi_2$ phase is not detected after annealing at 873 K nor at higher temperature. Secondly, the La_2O_3 diffraction peak which appears upon annealing at 1173 K near $2\theta \approx 32$ has a higher intensity. This confirms the presence of a greater amount of La_2O_3 resulting from the silicon depletion of the coating by diffusion towards the stainless steel substrate.

Fig. 4d shows the XRD pattern of the as-deposited La-Si film with a Si/(Si+La) ratio of 43.2% and its structure evolution with annealing temperature. As observed for the films deposited with higher Si contents, the as-deposited film has a quasi-amorphous structure and a broad peak centred around $2\theta = 33$ is detected after annealing up to 973 K. The La_2O_3 phase which was only detected at 1173 K in the films with higher Si content is obtained upon annealing at 873 K. Finally, the

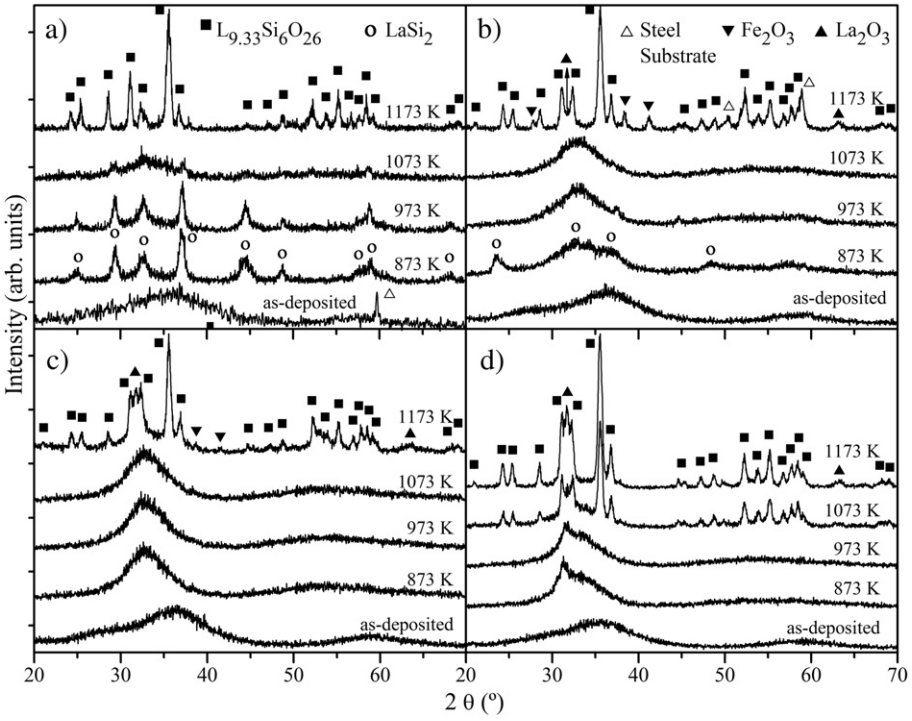

Fig. 4. X-ray diffraction patterns from the La-Si films with different Si/(Si+La) atomic ratios as a function of annealing temperature: a) 59.3%, b) 49%, c) 45.6% and d) 43.2%.

presence of lanthanum silicate apatite-like phase is detected at a lower annealing temperature (1073 K) as compared with the films deposited with higher Si content.

4. Discussion

The silicon content in the as-deposited films has no obvious effect on their structure: a quasi-amorphous structure was systematically obtained and characterized by a broad diffraction peak around $2\theta \approx 36$. The $LaSi_2$ phase is the only thermodynamically stable compound of the La-Si phase diagram detected upon annealing. This phase is formed only after the annealing of the films with higher Si contents (Si/(Si+La)>49%) at intermediate temperature. The corresponding temperature domain where $LaSi_2$ phase is formed decreases with increasing the Si content of the film: with Si/(La+Si) of 59.3%, $LaSi_2$ crystallises around 873 K and disappears around 1073 K, whereas for 49% Si, $LaSi_2$ crystallises very finely around 873 K and only a small amount is still present at 973 K. Decreasing the Si content into the La-Si as-deposited coating at 45.6% leads to the formation of an amorphous structure, instead of the $LaSi_2$ phase, which remains up to the full crystallisation of the films at 1173 K. For the as-deposited film containing the lower Si content (43.2%), the first phase which crystallises around 873 K is La_2O_3. Lanthanum oxide then remains stable even after the crystallisation of the apatite-like lanthanum silicate at 1173 K.

A striking feature of the annealing experiments is the systematic amorphisation of the films just before the crystallisation of the apatite-like lanthanum silicate structure at 1173 K. This amorphisation which occurs around 1073 K for the coating containing higher Si content (Si/(Si+La)=59.3%) is visible from 873 K for the other coatings, either together with $LaSi_2$ (Si/(Si+La)=49%) or with La_2O_3 (Si/(Si+La)= 43.2%). The amorphisation of crystalline phases by introducing oxygen into sputter-deposited coatings has already been observed [19,20] and clearly derives from the confusion principle related to the glass formation ability of materials constituted with elements of different atomic radii [21,22]. The displacement of the position of the main broad diffraction peak from $2\theta \approx 36$ for the as-deposited La-Si coatings toward lower Bragg angles ($2\theta \approx 33$) is representative of an increase of the average distance between first neighbour atoms in the amorphous phase [23] and is clearly related to the oxidation process, as already been observed elsewhere [20].

The lanthanum silicate apatite-like phase was obtained upon annealing at 1173 K for all the films studied. The annealing temperature required for $La_{9.33}Si_6O_{26}$ formation decreases with Si content as this phase was already detected after annealing the film with a Si/(Si+La) atomic ratio of 43.2% at 1073 K (see Fig. 4d). However, quite pure $La_{9.33}Si_6O_{26}$ was obtained only after the annealing of the film with the highest Si content (see Fig. 4a). For the other films, La_2O_3 is always detected when the lanthanum silicate phase is formed, with an increasing fraction and a decreasing crystallization temperature while decreasing the Si content of the as-deposited film. The presence of this phase in the annealed coatings, regardless of the fact that all the La-Si as-deposited coatings systematically present a Si/(Si+La) atomic ratio higher than that theoretically required to produce the lanthanum silicate, (~39%), is clearly related to the strong diffusion of silicon into the stainless steel substrate during annealing treatments.

5. Conclusions

Thin La-Si films were deposited by magnetron sputtering from pure La and Si targets. The Si/(Si+La) atomic ratio in the films was varied from 43.2 to 59.3%. The films have a homogeneous chemical composition down to the substrate and sharp interfaces. Annealing promotes the diffusion of the different species from the film to the substrate and vice-versa, resulting in the broadening of the interfaces.

X-Ray diffraction showed that all the as-deposited films had an amorphous structure. The formation of the $LaSi_2$ phase at intermediate temperatures was observed for the films deposited with higher Si contents while the films deposited with lower Si contents remained amorphous, eventually with a small amount of crystallized lanthanum oxide, up to the start of the apatite phase crystallization process. The lanthanum silicate apatite-like phase ($La_{9.33}Si_6O_{26}$) was obtained only after annealing at 1173 K, excepted for the film with lower Si content which was already partially crystallized after annealing at 1073 K. Quite pure $La_{9.33}Si_6O_{26}$ was obtained after annealing the film with the highest Si content (Si/(Si+La)=59.3%) although the theoretical Si/(Si+La) atomic ratio for apatite structure lanthanum silicate is only 39%. For the other films, La_2O_3 was always detected when the lanthanum silicate phase was formed. Both phenomena clearly result from the strong diffusion of silicon excess towards the stainless steel substrate.

Although the lanthanum silicate phase was obtained after oxidation of the deposited La-Si films, silicon diffusion into the substrate may prevent their application as SOFCs electrolytes. Further work using SOFCs anodes (such as Ni-YSZ cermets) as substrates and lower Si contents in the sputtered films will be carried out in order to establish the potential of the as synthesized films as SOFCs electrolytes.

Acknowledgements

The authors acknowledge the CAPM (Communeauté d'Agglomération du Pays de Montbéliard) and FCT (Fundação para a Ciência e a Tecnologia) for the financial support to LERMPS and SEG-CEMUC, respectively. The authors also acknowledge Sylvain Weber for the SNMS analyses.

References

[1] P. Singh, N.Q. Minh, Int. J. Appl. Ceram. Technol. 1 (2004) 5.
[2] M. Haile, Acta Mater. 51 (2003) 5981.
[3] E. Ivers-Tiffe'e, A. Weber, D. Herbstritt, J. Eur. Ceram. Soc. 21 (2001) 1805.
[4] V.V. Kharton, F.M.B. Marques, A. Atkinson, Solid State Ionics 174 (2004) 135.
[5] S.P.S. Badwal, K. Foger, Ceram. Int. 22 (1996) 257.
[6] L.R. Pederson, P. Singh, X.D. Zhou, Vacuum 80 (2006) 1066.
[7] P. Briois, F. Lapostolle, V. Demange, E. Djurado, A. Billard, Surf. Coat. Technol. 201 (2007) 6012.
[8] O. Yamamoto, Electrochim. Acta 45 (2000) 2423.
[9] P. Briois, A. Billard, Surf. Coat. Technol. 201 (2006) 1328.
[10] C. Brahim, A. Ringuedé, E. Gourba, M. Cassir, A. Billard, P. Briois, J. Power Sources 156 (2006) 45.
[11] S. Nakayama, M. Sakamoto, J. Eur. Ceram. Soc. 18 (1998) 1413.
[12] P.R. Slater, J.E.H. Sansom, J.R. Tolchard, Chem. Rec. 4 (2004) 373.
[13] P. Briois, F. Lapostolle, A. Billard, Plasma Proc. Polym. 14 (2007) 99.
[14] V. Rachpech, PhD thesis, École des Mines de Nancy, France, 2007.
[15] H. Nakano, S. Yamanaka, J. Solid State Chem. 108 (1994) 260.
[16] M.V. Bulanova, P.N. Zheltov, K.A. Meleshevich, P.A. Saltykov, G. Effenberg, J.C. Tedenac, J. Alloys Compd. 329 (2001) 214.
[17] U. Kolitsch, H. Seifert, F. Aldinger, J. Solid State Chem. 120 (1995) 38.
[18] J. Felsche, Naturwissenchafyen 56 (1969) 212.
[19] J.F. Pierson, A. Billard, T. Belmonte, H. Michel, C. Frantz, Thin Solid Films 347 (1999) 78.
[20] P. Gutier, A. Darbeïda, A. Billard, C. Frantz, J. von Stebut, Surf. Coat. Technol. 114 (1999) 148.
[21] J. Basu, S. Ranganathan, Acta Mater. 54 (2006) 3637.
[22] D.B. Miracle, O.N. Senkov, W.S. Sanders, K.L. Kendig, Mater. Sci. Eng., A 375–377 (2004) 150.
[23] F. Sanchette, A. Billard, C. Frantz, Surf. Coat. Technol. 98 (1998) 1162.